AGU PUBLICATIONS

Tectonics

RESEARCH ARTICLE
10.1002/2016TC004170

Key Points:
- New Carboniferous and Permian ophiolites have been documented in central Qiangtang, Tibet
- The LSSZ represent the main suture of the Paleo-Tethys Ocean which existed and evolved from Devonian to Triassic
- The opening and demise of the Paleo-Tethys Ocean dominated the formation of the major framework for the East and/or Southeast Asia

Supporting Information:
- Supporting Information S1

Correspondence to:
X.-Z. Zhang and Q. Wang,
zhangxz@gig.ac.cn;
wqiang@gig.ac.cn

Citation:
Zhang, X.-Z., Y.-S. Dong, Q. Wang, W. Dan, C. Zhang, M.-R. Deng, W. Xu, X.-P. Xia, J.-P. Zeng, and H. Liang (2016), Carboniferous and Permian evolutionary records for the Paleo-Tethys Ocean constrained by newly discovered Xiangtaohu ophiolites from central Qiangtang, central Tibet, *Tectonics*, *35*, 1670–1686, doi:10.1002/2016TC004170.

Received 8 MAR 2016
Accepted 30 JUN 2016
Accepted article online 3 JUL 2016
Published online 18 JUL 2016

Carboniferous and Permian evolutionary records for the Paleo-Tethys Ocean constrained by newly discovered Xiangtaohu ophiolites from central Qiangtang, central Tibet

Xiu-Zheng Zhang[1], Yong-Sheng Dong[2], Qiang Wang[1,3], Wei Dan[1,3], Chunfu Zhang[4], Ming-Rong Deng[2], Wang Xu[2], Xiao-Ping Xia[1], Ji-Peng Zeng[1], and He Liang[1]

[1]State Key Laboratory of Isotope Geochemistry, Guangzhou Institute of Geochemistry, Chinese Academy of Sciences, Guangzhou, China, [2]College of Earth Science, Jilin University, Changchun, China, [3]CAS Center for Excellence in Tibetan Plateau Earth Science, Beijing, China, [4]Department of Geosciences, Fort Hays State University, Hays, Kansas, USA

Abstract Reconstructing the evolutionary history of the Paleo-Tethys Ocean remains at the center of debates over the linkage between Gondwana dispersion and Asian accretion. Identifying the remnants of oceanic lithosphere (ophiolites) has very important implications for identifying suture zones, unveiling the evolutionary history of fossil oceans, and reconstructing the amalgamation history between different blocks. Here we report newly documented ophiolite suites from the Longmu Co-Shuanghu Suture zone (LSSZ) in the Xiangtaohu area, central Qiangtang block, Tibet. Detailed geological investigations and zircon U-Pb dating reveal that the Xiangtaohu ophiolites are composed of a suite of Permian (281–275 Ma) ophiolites with a nearly complete Penrose sequence and a suite of Early Carboniferous (circa 350 Ma) ophiolite remnants containing only part of the lower oceanic crust. Geochemical and Sr-Nd-O isotopic data show that the Permian and Carboniferous ophiolites in this study were derived from an N-mid-ocean ridge basalts-like mantle source with varied suprasubduction-zone (SSZ) signatures and were characterized by crystallization sequences from wet magmas, suggesting typical SSZ-affinity ophiolites. Permian and Carboniferous SSZ ophiolites in the central Qiangtang provide robust evidence for the existence and evolution of an ancient ocean basin. Combining with previous studies on high-pressure metamorphic rocks and pelagic radiolarian cherts, and with tectonostratigraphic and paleontological data, we support the LSSZ as representing the main suture of the Paleo-Tethys Ocean which probably existed and evolved from Devonian to Triassic. The opening and demise of the Paleo-Tethys Ocean dominated the formation of the major framework for the East and/or Southeast Asia.

1. Introduction

Paleo-Tethys is widely accepted as an Early Devonian to Triassic ocean which was initially opened in response to the detachment of the "Asiatic Hunic superterrane" from the northern margin of Gondwana and eventually closed as a result of the collision between Gondwana affinity blocks and Eurasia [*Li*, 1987; *Li et al.,* 1995, 2006; *Stampfli and Borel*, 2002; *von Raumer et al.,* 2002; *Ferrari et al.,* 2008; *Lehmann et al.,* 2013; *Metcalfe*, 1994, 2013; *Yin and Harrison*, 2000; *Zhai et al.,* 2011a, 2011b, 2013; *Zhang et al.,* 2014a, 2014b, 2014c]. Its evolution largely dominates our knowledge of the origin and early formation of the East and/or Southeast Asia (reviewed by *Metcalfe* [2013]). Hence, identifying the remnants of the main Paleo-Tethys Ocean and unveiling its evolutionary history have always been hot topics, and they remain at the center of debates [*Metcalfe*, 1994, 2013; *Yin and Harrison*, 2000; *Zhai et al.,* 2011a, 2011b, 2013; *Zhang et al.,* 2014a, 2014b, 2014c].

Previous studies suggest that a $>$ 500 km long east-west trending tectonic mélange belt named the Longmu Co-Shuanghu Suture zone (LSSZ) (Figure 1) should be a key locality to investigating the evolution of the Paleo-Tethys Ocean [*Li*, 1987; *Li et al.,* 1995; *Metcalfe*, 1994, 2013]. The LSSZ is composed of low-temperature-high-pressure (LT-HP) metamorphic rocks (eclogites and blueschists), ophiolites, oceanic island basalts (OIB)-type basalts, metasedimentary rocks, and minor cherts [*Kapp et al.,* 2000, 2003; *Li et al.,* 2006, 2008; *Zhu et al.,* 2006; *Pullen et al.,* 2008; *Zhang et al.,* 2006a, 2006b; *Tang and Zhang*, 2014; *Zhai et al.,* 2011a, 2011b, 2013; *Zhang et al.,* 2014b]. Previous studies focused on LT-HP metamorphic rocks [*Kapp et al.,* 2000, 2003; *Li et al.,* 2006; *Zhang et al.,* 2006a, 2006b; *Pullen et al.,* 2008; *Zhai et al.,* 2011a, 2011b; *Zhang et al.,* 2014b] and two competing models have been proposed to account for their formation: (1) in situ suture of

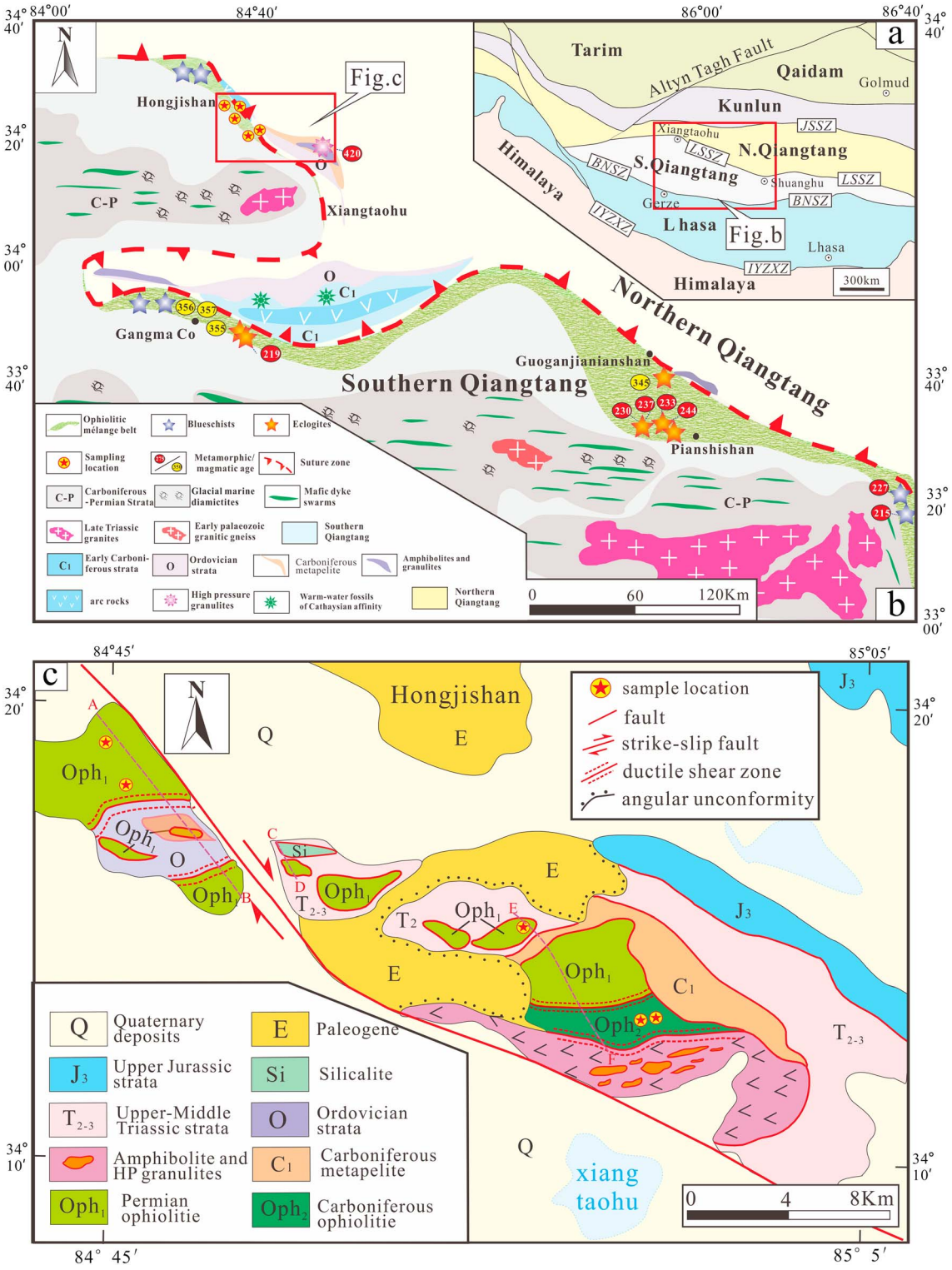

Figure 1. (a) Sketch map of Tibet (modified after *Zhai et al.* [2011a]), showing the distributions of the main suture zones. (b) Simplified geological map of the Qiangtang area, central Tibet (modified from *Zhang et al.* [2014a]). (c) Geologic map of the Xiangtaohu areas, showing outcrops of the ophiolites and the sample locations for zircon dating. The dashed lines (AB, CD, and EF) are cross sections of ophiolites (Figure S1 in the supporting information). JSSZ = Jinsha Suture Zone, LSSZ = Longmu Co-Shuanghu Suture Zone, BNSZ = Bangong-Nujiang Suture Zone, and IYZSZ = Indus-Yarlung Zangbo Suture Zone. The metamorphic and magmatic ages are from *Zhai et al.* [2011a, 2013], *Deng et al.* [2000], *Pullen et al.* [2008], and *Zhang et al.* [2014a].

the main Paleo-Tethys Ocean relic [*Li*, 1987; *Li et al.,* 1995, 2008; *Zhai et al.,* 2011a, 2011b, 2013; *Metcalfe*, 2013]; and (2) low-angle southward subduction of the Songpan-Ganzi accretionary mélange along the Jinsha suture [*Kapp et al.,* 2000; *Pullen et al.,* 2011].

The dispute stems mainly from the limited systematic studies on ophiolites in the Longmu Co-Shuanghu area, which were thought to have constituted the crucial geological archives of ancient oceanic lithosphere and have important implications for identifying the suture zone and unveiling the evolutionary history of fossil oceans [e.g., *Coleman*, 1977; *Dewey and Bird*, 1971; *Dilek*, 2003]. Moreover, most of the ophiolites reported along the LSSZ have been determined to have been formed in the Early Paleozoic [*Li et al.,* 2008; *Zhai et al.,* 2010; *Hu et al.,* 2014; *Zhai et al.,* 2016], which are too old to unveil the evolutionary history of the Paleo-Tethys Ocean (reviewed by *Metcalfe* [2013]).

In this contribution, we report newly documented ophiolite suites in the Xiangtaohu area of the central Qiangtang block, Tibet. These suites occur in the LSSZ, and our new SHRIMP (sensitive high-resolution ion microprobe) and LA-ICP-MS (laser ablation inductively coupled plasma mass spectrometry) U-Pb zircon age dating suggests they were generated in Early Permian (281–275 Ma) and Early Carboniferous (circa 350 Ma). This provides robust evidence for the existence and evolution of the Paleo-Tethys Ocean in the central Qiangtang block.

2. Geological Setting

Tibet is composed of several continental blocks (Figure 1a) that progressively accreted to Asia as a result of the closure of the intervening Tethyan oceans (Paleo- to Ceno-Tethys) throughout the Paleozoic to Mesozoic [*Yin and Harrison*, 2000; *Metcalfe*, 2013]. The Qiangtang block is situated in the central part of the Tibetan Plateau, which is bounded by the Jinsha suture zone to the north and the Bangong-Nujiang suture to the south (Figures 1a and 1b) [*Yin and Harrison*, 2000]. Recent studies subdivided the Qiangtang block into the northern and southern Qiangtang blocks (NQB and SQB) with different affinities by LSSZ [*Li*, 1987; *Li and Zheng*, 1993; *Zhang et al.,* 2006b; *Zhai et al.,* 2011a, 2011b, 2013; *Metcalfe*, 2013]. To the north side of the LSSZ, the NQB consists of Late Devonian to Triassic sedimentary sequences overlain by Jurassic to Cenozoic sedimentary rocks [*Li and Zheng*, 1993; *Li et al.,* 1995]. Some Late Paleozoic sedimentary rocks contain abundant warm-water fossils of a Cathaysian affinity [*Li and Zheng*, 1993; *Li et al.,* 1995; *Zhang et al.,* 2009; *Peng et al.,* 2014]. In contrast, the SQB is characterized by Carboniferous to Permian glaciomarine deposits with cold-water biota, which are typical indicators of a Gondwanan affinity [*Li and Zheng*, 1993; *Li et al.,* 1995; *Metcalfe*, 1994; *Fan et al*., 2014].

The LSSZ, first proposed by *Li* [1987] as an in situ Triassic suture zone (Figures 1a and 1b), is composed of blueschists, eclogites, ophiolites, OIB-type basalts, metasedimentary rocks, and minor chert [*Li et al.,* 1995, 2006, 2008; *Kapp et al.,* 2000, 2003; *Zhang et al.,* 2014b; *Zhai et al.,* 2011a, 2011b, 2013], and it continues to be regarded as the relic of the main Paleo-Tethys Ocean [*Zhai et al.,* 2011a, 2011b, 2013; *Zhu et al.,* 2013; *Metcalfe*, 2013]. The cumulate gabbros in the Gangma Co and Guoganjianian areas yielded ages (SHRIMP) of 357–355 Ma and circa 345 Ma, respectively [*Zhai et al.,* 2013]. The timing of high-pressure/low-temperature metamorphism has been constrained as Middle to Late Triassic based on Lu-Hf isochron dating of the eclogites and blueschists (244–223 Ma) [*Pullen et al.,* 2008] and U-Pb zircon (SHRIMP) dating of the eclogites (237–230 Ma) [*Zhai et al.,* 2011a].

3. Field Occurrence and Rock Characteristics

The ophiolites from the Xiangtaohu area (Figures 1b and 1c) are distributed in a ~25 km long by ~8 km wide, NE-SW trending belt, and are in fault contact with the Ordovician to Triassic metasedimentary rocks and the Early Paleozoic high-pressure granulites and amphibolites (Figure 1b) [*Zhang et al.,* 2014a]. Based on detailed geological investigations, the Xiangtaohu ophiolites were proved to be an ophiolitic complex containing two suites of ophiolite remnants (Figures 1c and S1 in the supporting information). One suite (Oph_1) is widely distributed in the Xiangtaohu area and includes a nearly complete "Penrose sequence" (upper mantle peridotite, lower crust layered ultramafic to mafic cumulate rocks, upper crust sheeted dykes, pillow lavas, and deep-marine cover sediments) (as defined by *Penrose Conference Participants* [1972]). It is mainly composed of serpentinized peridotites, metamorphic cumulate gabbros, metagabbros, metabasalts, metadiabases, and minor metasilicalite (Figures 2a–2d), but without the typical sheeted dikes. Most of these rocks have

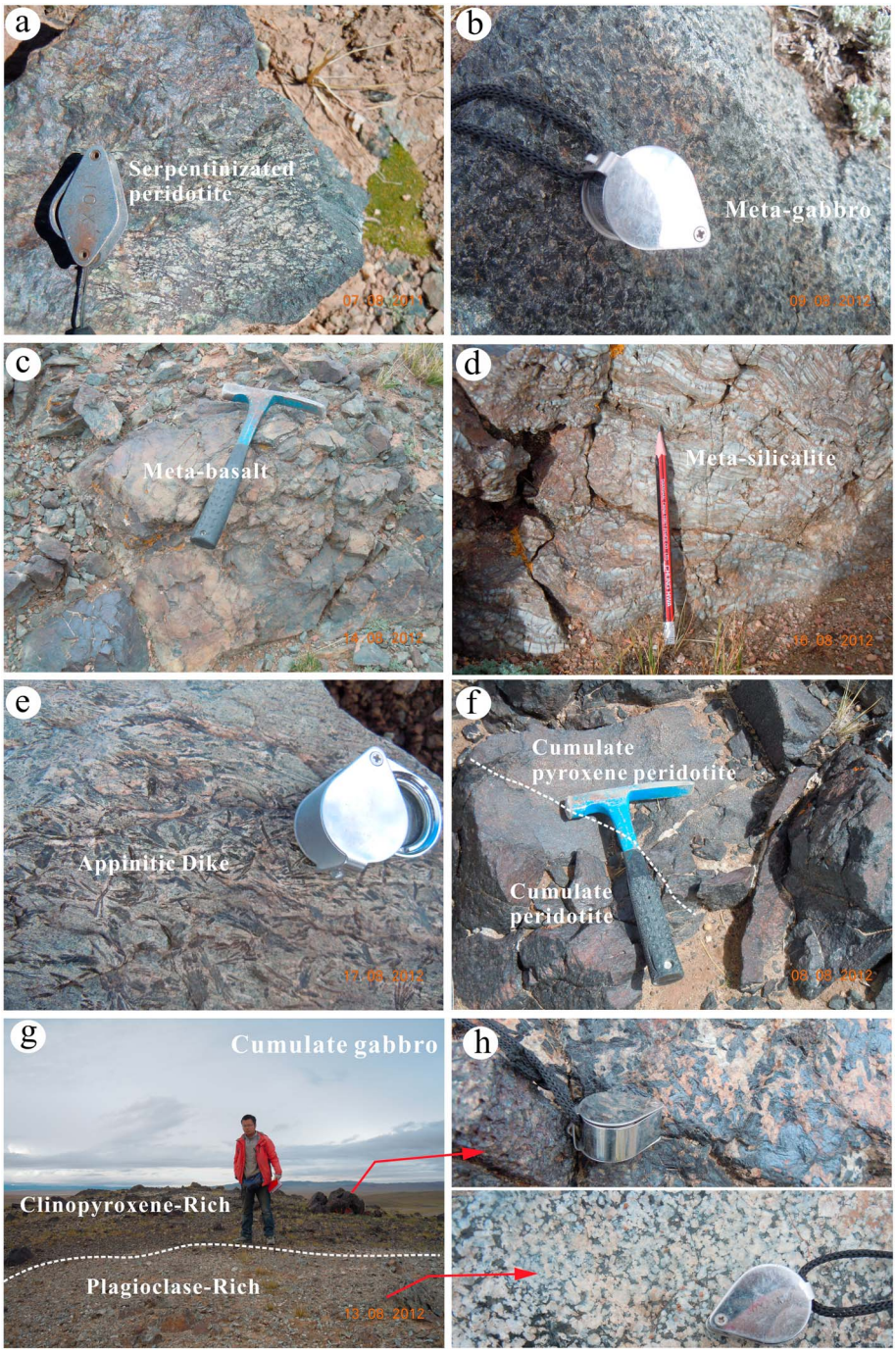

Figure 2. Field photographs showing the occurrences of the ophiolites from the Xiangtaohu area, central Qiangtang block. (a–e) Occurrences of serpentinized peridotites, metagabbros, metabasalts, metasilicalite, and appinitic dikes from the Permian ophiolites (Oph_1). (f–h) Occurrences of a suite of lower crust layered ultramafic to mafic cumulate rocks from the Early Carboniferous ophiolites (Oph_2).

undergone greenschist-facies metamorphism and variable degrees of deformation (Figures 3a–3d). The olivines in the ultramafic rocks have been almost completely altered to serpentine (Figure 3a), and the pyroxenes in the mafic rocks have generally been replaced by chlorite, actinolite, and epidote (Figures 3b and 3c). Some plagioclase grains in the metagabbros have experienced saussuritization and have been changed to albite + zoisite symplectites (Figures 3b and 3e). In addition to the primary rock types mentioned above, we also discovered some special appinitic dikes (Figures 2e and 3e), which are an important

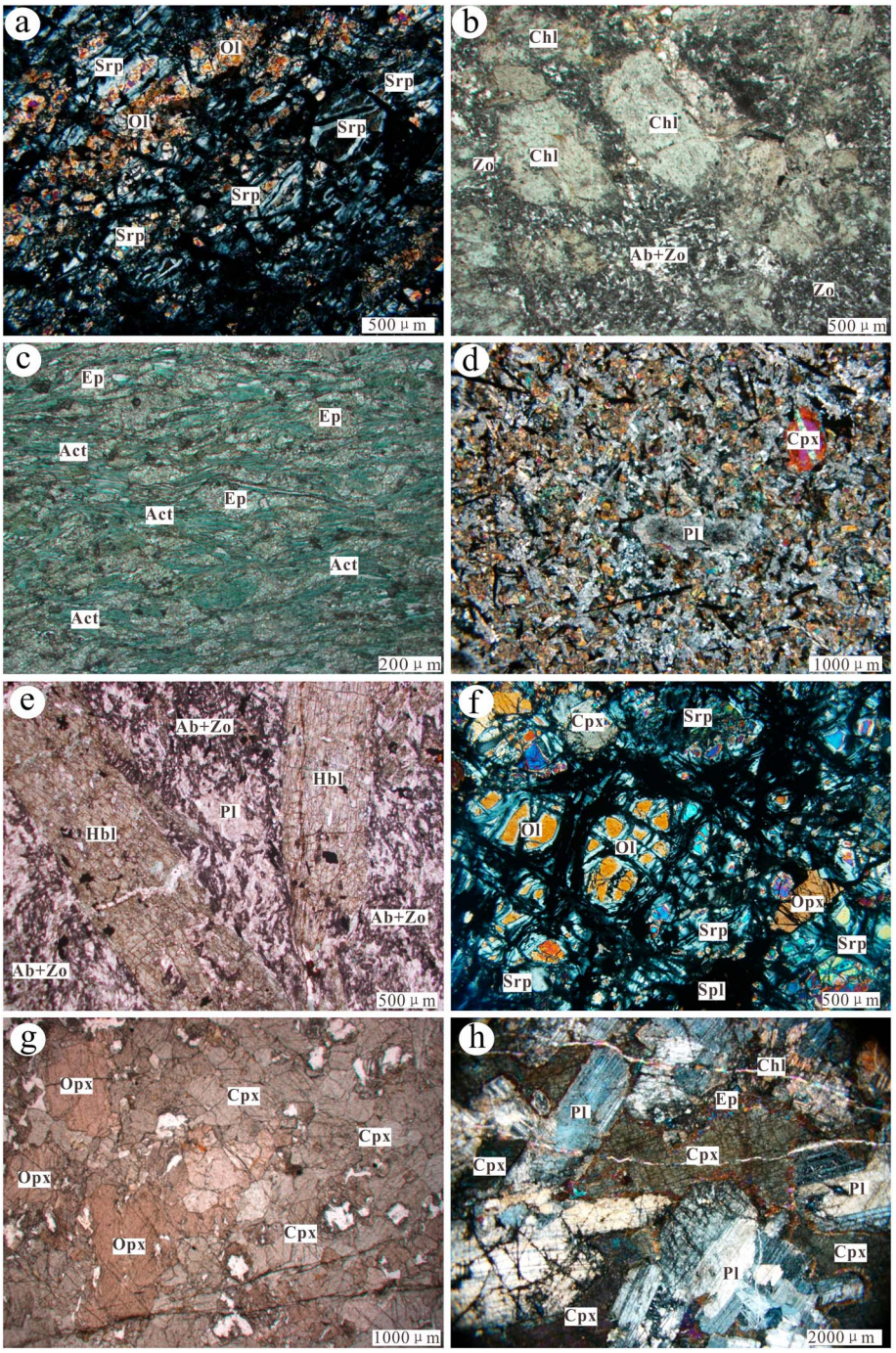

Figure 3. Photomicrographs showing mineral textures and assemblages in the Xiangtaohu ophiolites from the central Qiangtang block, central Tibet. (a–e) Photomicrographs of the Permian ophiolites (Oph_1) suggest that most of these rocks have undergone greenschist-facies metamorphism and variable degrees of deformation. (f–h) Photomicrographs of the Early Carboniferous ophiolites (Oph_2) show that these rocks are unfoliated and have only experienced slight epidotization and chloritization. Notes: Figures 3a, 3d, 3f, and 3h are crossed polarized light photomicrographs, and the rest of figures are plane polarized light photomicrographs. Mineral abbreviations: Cpx-clinopyroxene, Ol-olivine, Opx-orthopyroxene, Hbl-hornblende, Pl-plagioclase, Srp-serpentine, Chl-chlorite, Act-actinolite, Ep-epidote, and Ab-albite, Zo-zoisite.

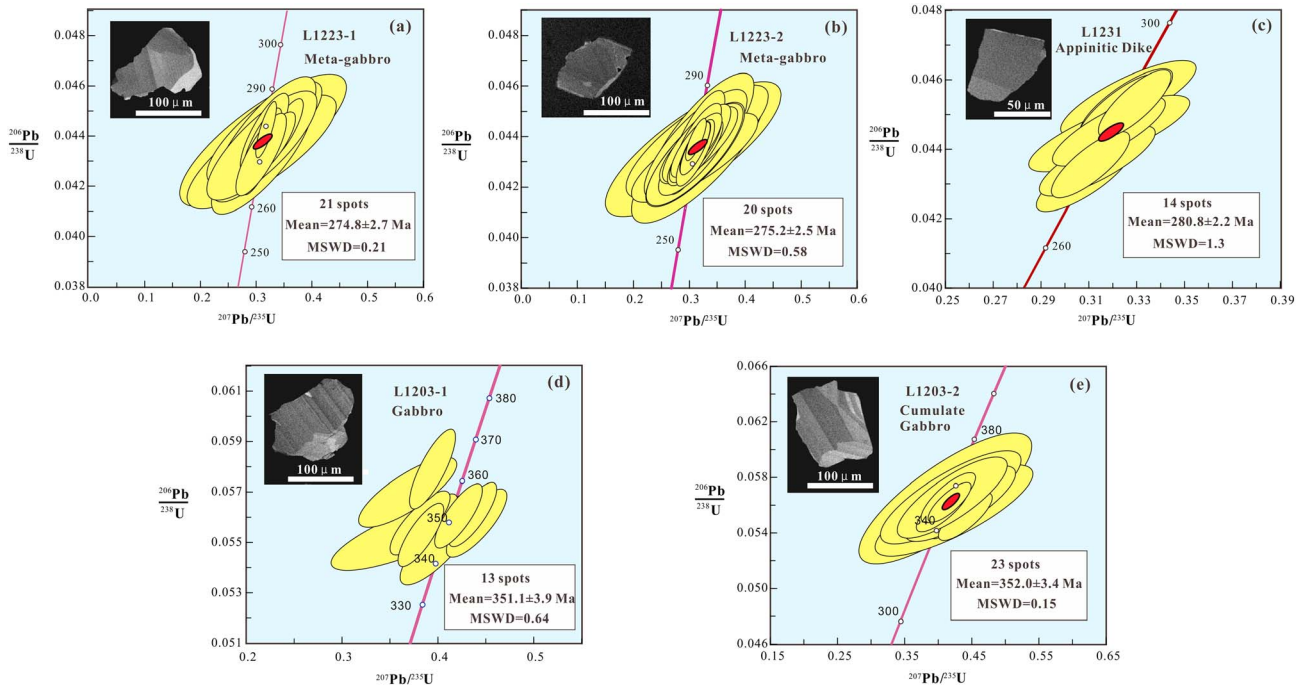

Figure 4. Zircon U-Pb concordia diagrams and CL images for the Xiangtaohu ophiolites from the central Qiangtang block, central Tibet. (a–c) Metagabbros, metamorphic cumulate gabbro, and appinitic dike from Oph_1. (d and e) Gabbro and cumulate gabbro from Oph_2.

constituent of suprasubduction-zone (SSZ) ophiolites and require water-bearing magmas [*Metcalf and Shervais*, 2008]. These rocks occurred as small intrusions in metabasalts (Figure S2a and S2b in the supporting information) and are mainly mafic in composition. They are characterized by euhedral and centimeter-scale hornblende crystals in the matrix (Figures 2e and 3e) and underwent greenschist-facies metamorphism. Only a few hornblendes of magmatic origin in the appinitic dikes were retained (Figure 3e), and most hornblende grains occurred as residual cores or have been completely replaced by actinolites (Figures S2c–S2f).

Another suite of ophiolite remnants (Oph_2) is only localized in the southeast of the Xiangtaohu area and contacts with the Oph_1 to the north and Early Paleozoic amphibolites to the south by faults (Figures 1c and S1). The suite of Oph_2 contains limited rock types and consists of lower crust layered ultramafic to mafic cumulate rocks, including cumulate pyroxene peridotite, cumulate pyroxenite, cumulate gabbro, and gabbro (Figures 2f–2h). Compared to Oph_1, most rocks from Oph_2 are unfoliated and have only experienced slight epidotization and chloritization (Figures 3f–3h).

4. Analytical Methods and Results

Analytical methods are described in Text S1 in the supporting information. The zircon U-Pb data, whole rock major and trace elements, Sr-Nd isotope, and zircon O isotope data for the Xiangtaohu ophiolites are listed in Tables S1–S4, respectively, in the supporting information.

4.1. Zircon U-Pb Dating Results

Representative metagabbro samples (L1223-1 and L1223-2) and an appinitic dike sample (L1231) from Oph_1 were selected for LA-ICP-MS zircon U-Pb analyses (Table S1 and Figure 4). Zircon grains from these samples are euhedral and colorless with average crystal lengths of 80–200 μm and length-to-width ratios of ~2:1. The cathodoluminescence (CL) images of zircons exhibit a broad-spaced zoning texture (Figures 4a–4c). The analyzed zircon grains have highly variable U (9–761 ppm) and Th (6–1005 ppm) contents, with Th/U ratios of 0.43–2.74 (Table S1). These features suggest that the zircons are of magmatic origin [*Hoskin and Black*, 2000]. The two metagabbro samples (L1223-1 and L1223-2) yielded similar weighted mean $^{206}Pb/^{238}U$ ages of 274.8 ± 2.7 Ma (mean square weighted deviation MSWD = 0.21) and 275.2 ± 2.5 Ma (MSWD = 0.58)

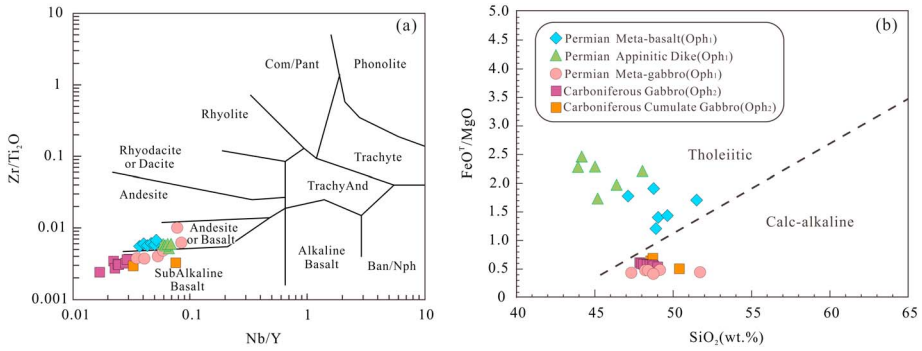

Figure 5. (a) Zr/TiO_2 versus Nb/Y diagram distinguishing subalkaline and alkaline basalts [*Winchester and Floyd*, 1977]. (b) FeO^T/MgO versus SiO_2 diagram distinguishing tholeiitic and calc-alkaline series [*Miyashiro*, 1974].

(Figures 4a and 4b). The appinitic dike sample (L1231) yielded a weighted mean $^{206}Pb/^{238}U$ age of 280.8 ± 2.2 Ma (MSWD = 1.3) (Figure 4c).

Representative samples of gabbro (L1203-1) and cumulate gabbro (L1203-2) from Oph_2 were selected for zircon dating using the SHRIMP II and LA-ICP-MS methods (Table S1 and Figure 4), respectively. Zircon grains from samples L1203-1 and L1203-2 have similar features of crystal habit and CL images as those from Oph_1 (Figures 4d and 4e). Most zircon grains analyzed have highly variable U (43–686 ppm) and Th (16–486 ppm), with Th/U ratios of 0.22–2.19 (Table S1), implying that they are of magmatic origin [*Hoskin and Black*, 2000]. Samples L1203-1 and L1203-2 yielded similar weighted mean $^{206}Pb/^{238}U$ ages of 351.1 ± 3.9 Ma (MSWD = 0.64) and 352.0 ± 3.4 Ma (MSWD = 0.15) (Figures 4d and 4e), respectively.

4.2. Major and Trace Element Compositions

Thirty-one whole-rock samples from Oph_1 and Oph_2 in the Xiangtaohu area are selected for major and trace element analyses. These samples include five metabasalt, six metagabbro, and five appinitic dike samples from Oph_1, and eight gabbro, two cumulate gabbro, and five fresh cumulate pyroxene peridotite samples from Oph_2.

The metabasalt samples from Oph_1 display variable SiO_2 contents ranging from 47.1 to 51.5 wt % and are characterized by moderate TiO_2 contents (1.26–1.89 wt %), relatively low Al_2O_3 contents (13.7–14.6 wt %), and relatively high FeO^T contents (9.91–12.4 wt %). The appinitic dike samples from Oph_1 have SiO_2 (43.9–46.4 wt %), TiO_2 (1.08–1.26 wt %), and FeO^T contents (8.74–10.19 wt %) similar to the metabasalt samples but have relatively higher Al_2O_3 contents (20.0–21.9 wt %). In contrast, the mafic samples from the lower crust of both Oph_1 and Oph_2 (gabbro and cumulate gabbro) have similar SiO_2 contents (47.3 to 51.7 wt %), much lower TiO_2 contents (0.12–0.26 wt %), higher Al_2O_3 contents (17.0–28.4 wt %), and lower FeO^T contents (1.73–4.64 wt %). In addition, we also selected some fresh ultramafic rock samples (cumulate pyroxene peridotites) for geochemical analyses and found that they are characterized by low SiO_2 contents (37.3–38.5 wt %), very high MgO (31.7–32.9 wt %), Cr (3759–4002 ppm), and Ni (1314–1430 ppm) contents.

The mafic rock samples from Oph_1 and Oph_2 have variable MgO (2.51–10.46 wt %) contents, $Mg^{\#}$ [100 × atomic MgO/(MgO + FeO)] values of 41–81 (Table S2), Cr concentrations of 51.9–881 ppm, and Ni contents of 55.4–197 ppm. On the Zr/TiO_2-Nb/Y diagram of *Winchester and Floyd* [1977], all the samples plot in the subalkaline basalt to andesite fields (Figure 5a). On the SiO_2-FeO^T/MgO diagram (Figure 5b), the metabasalt and appinitic dike samples from Oph_1 define a typical tholeiitic compositional trend, while the gabbro and cumulate gabbro samples from both Oph_1 and Oph_2 define a calc-alkaline trend.

The mafic to ultramafic rocks from Oph_1 and Oph_2 have highly variable total rare earth element (REE) contents (3.76–63.3 ppm) but display nearly uniform chondrite-normalized REE patterns. Apart from two cumulate gabbro samples (L1203-2 and L1203-3) with slightly enriched light rare earth elements (LREEs, $[La/Yb]_N = 2.26–2.77$) and positive Eu anomalies ($\delta Eu = 2.10–2.28$; $\delta Eu = Eu_N/\sqrt[2]{Sm_N \times Gd_N}$), most samples are characterized by obviously depleted to flat LREEs ($[La/Yb]_N = 0.29–1.21$) and relatively flat heavy REEs (HREEs, $[Gd/Yb]_N = 1.02–1.33$) with variable Eu anomalies ($\delta Eu = 0.69–1.46$) (Table S2 and Figures 6a, 6c, 6e, and 6g), which are mostly comparable with those of mid-ocean ridge basalts (N-MORB) [*Sun and McDonough*,

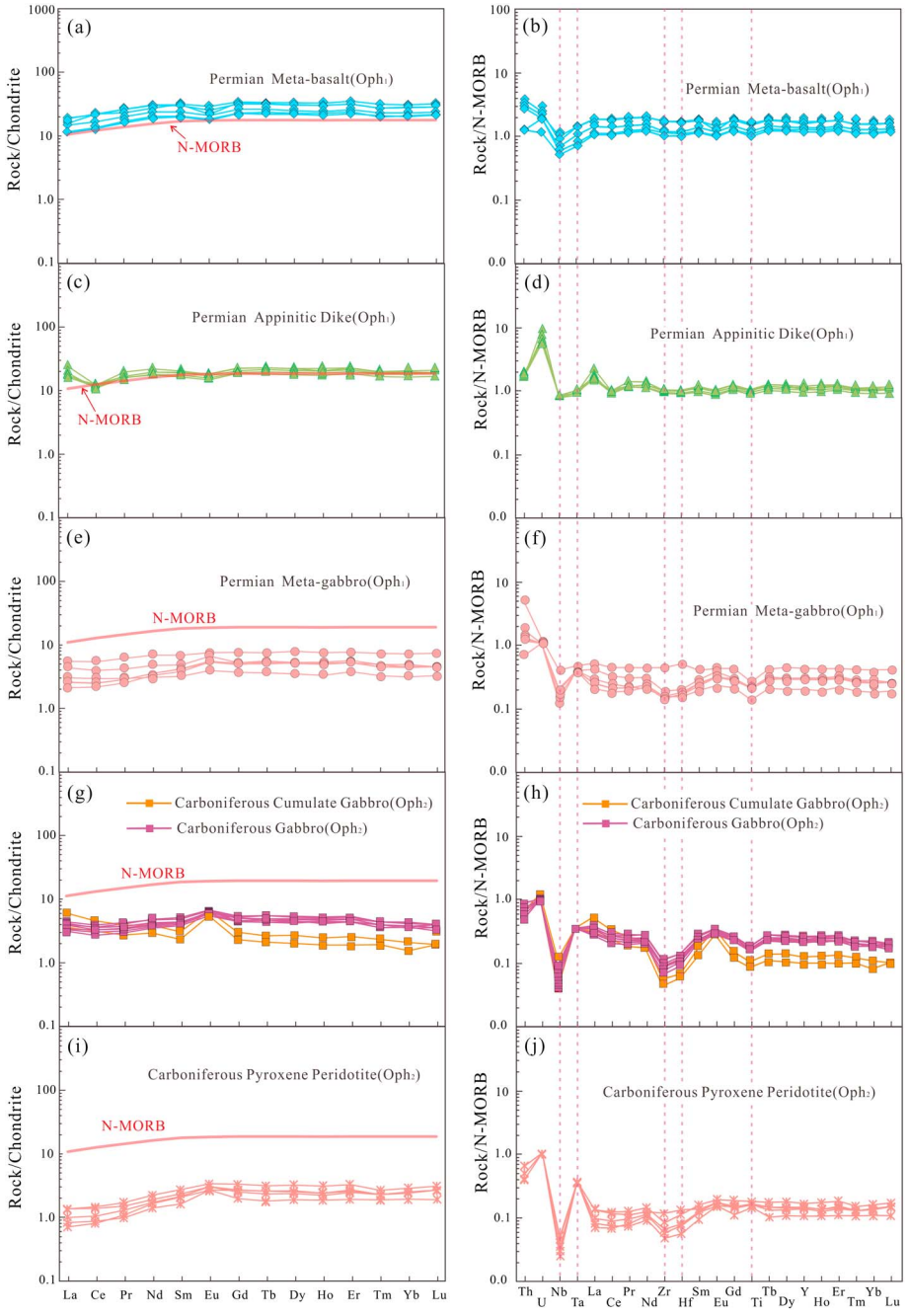

Figure 6. Chondrite-normalized REE distribution patterns and N-MORB-mantle normalized multielement plots for the (a–f) Permian ophiolites (Oph_1) and the (g–j) Early Carboniferous ophiolites (Oph_2) from the Xiangtaohu area, the central Qiangtang block, central Tibet. Chondrite and N-MORB values are from *Sun and McDonough* [1989].

1989]. Moreover, these samples have nearly horizontal N-MORB-normalized multielement patterns, slight enrichment in Th, and depletion in Nb and Ti to varying degrees (Figures 6b, 6d, 6f, and 6h).

4.3. Sr-Nd Isotope Compositions

Ten representative whole-rock samples were analyzed for Sr and Nd isotope compositions (Table S3 and Figure 7a). Most samples exhibit slightly variable initial $^{87}Sr/^{86}Sr$ ratios ranging from 0.7032 to 0.7051, except for two samples with higher initial $^{87}Sr/^{86}Sr$ ratios (0.7059 and 0.7061) which could have been modified by seawater hydrothermal alteration [e.g., *McCulloch et al.,* 1981; *Godard et al.,* 2006] or by some other

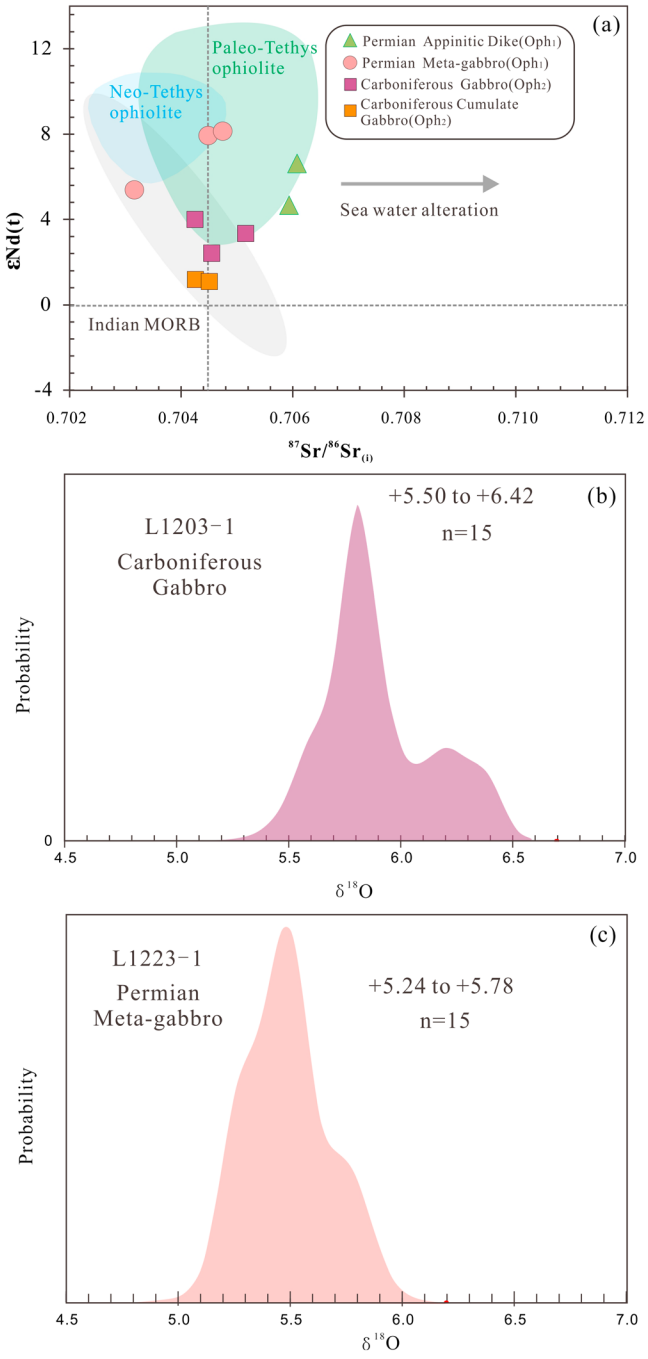

Figure 7. (a) $\varepsilon_{Nd}(t)$ versus ($^{87}Sr/^{86}Sr$) diagram for the Xiangtaohu ophiolites; (b and c) Histograms of zircon $\delta^{18}O_{zircon}$ values for the Xiangtaohu ophiolites in the central Qiangtang block, central Tibet. Data for the Paleo- and Neo-Tethys ophiolites are from *Xu and Castillo* [2004].

metamorphism(s) (Figure 8a). Moreover, all samples have positive $\varepsilon_{Nd}(t)$ values (Table S3), and the samples from Oph_1 have higher $\varepsilon_{Nd}(t)$ values (+4.67 to +8.15) than those of samples from Oph_2 (+1.12 to +4.08). On the $^{87}Sr/^{86}Sr$ versus $\varepsilon_{Nd}(t)$ diagram, all the ophiolitic rocks plot in the range of age-corrected Paleo- and Neo-Tethys ophiolites [*Xu and Castillo*, 2004].

4.4. Zircon O Isotopic Geochemistry

Two representative gabbro samples from both Oph_1 (L1223-1) and Oph_2 (L1203-1) were selected for in situ zircon O isotopic analyses. The results are listed in Table S4 and plotted in Figures 7b and 7c. The measured $\delta^{18}O$ values for zircons from L1223-1 show limited ranges of 5.2 to 5.8‰, forming a nearly normal Gaussian distribution, with an averaged value of 5.49 ± 0.18‰ (1σ). The sample L1203-1 has slightly variable measured $\delta^{18}O$ values ranging from 5.6‰ to 6.4‰, averaging 5.90 ± 0.24‰ (1σ). The zircon O isotope values of samples L1223-1 and L1203-1 are either within the range of those of igneous zircons in equilibrium with mantle magmas (5.3 ± 0.3‰) or slightly higher [*Valley*, 2003].

5. Discussion

5.1. Ages of Ophiolites in the Central Qiangtang Block

The Xiangtaohu ophiolites in this study include two suites, one is a nearly complete Penrose sequence (Oph_1) and the other is incomplete, containing only part of the lower oceanic crust (Oph_2). The metagabbro (L1223-1 and L1223-2) and appinitic dike (L1231) samples from Oph_1 yielded similar weighted mean $^{206}Pb/^{238}U$ ages of 281–275 Ma (Figures 4a–4c). These results indicate that the main part of the Xiangtaohu ophiolites (Oph_1) is a suite of Permian ophiolites, which is consistent with the occurrence of Permian pelagic radiolarian cherts in the Shuanghu area from LSSZ [*Zhu et al.*, 2006]. The gabbro (L1203-1) and cumulate gabbro (L1203-2) samples are remnants of the lower oceanic crust (Oph_2), yielding weighted mean $^{206}Pb/^{238}U$ ages of circa 350 Ma (Figures 4d and 4e), contemporary with the Carboniferous ophiolites in the Gangma Co (357–355 Ma) and Guoganjianianshan (345 Ma) along the LSSZ (Figure 1b) [*Zhai et al.*, 2013].

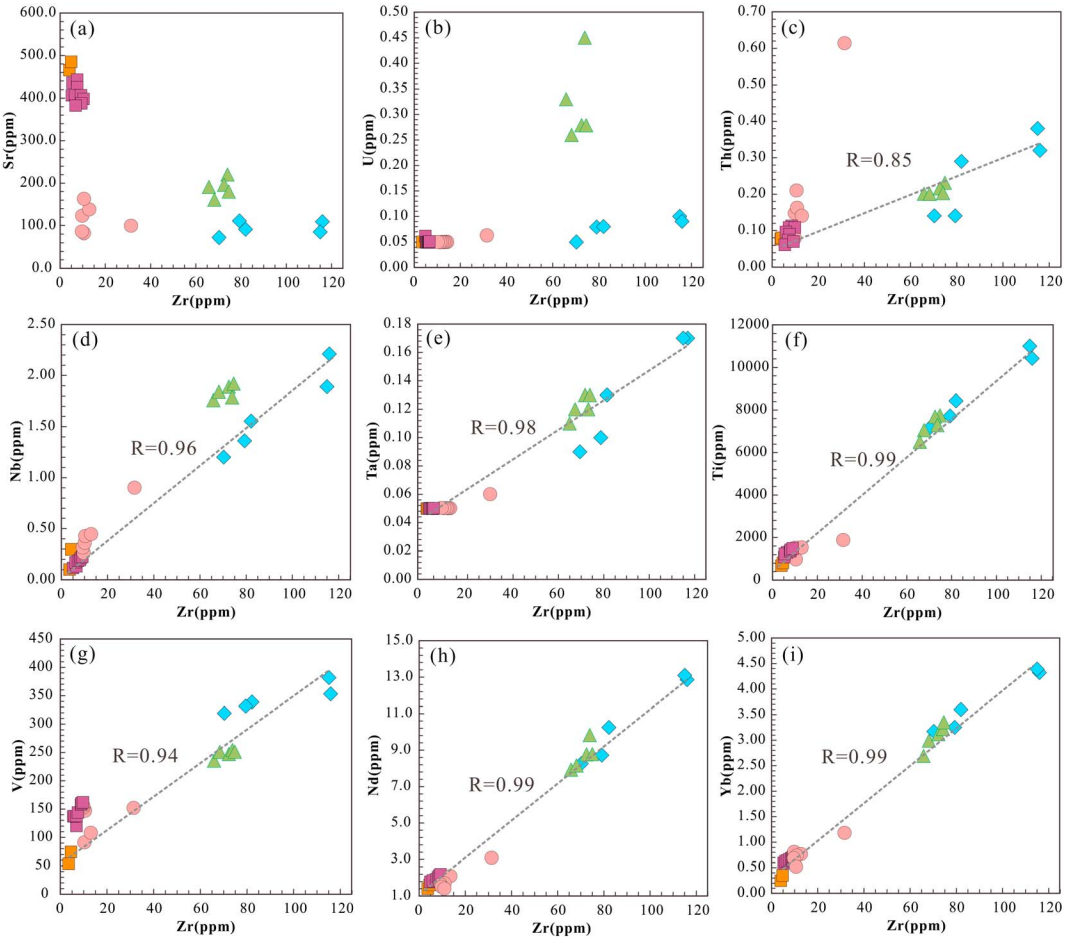

Figure 8. Zr versus selected element variation diagrams highlighting the effects of metamorphic alteration. The symbols are the same as in Figure 5.

In recent years, a growing number of Early Paleozoic oceanic crust remnants have been reported, including the Taoxinghu area (cumulate gabbro: 467 Ma) [*Zhai et al.,* 2010], the Gangma Co area (plagiogranites and gabbros: 505–437 Ma) [*Hu et al.,* 2014; *Zhai et al.,* 2016], and the Guogganjianianshan area (cumulate gabbro: 438 Ma) [*Li et al.,* 2008], all of which are located in the LSSZ (Figure 11a). *Zhai et al.* [2016] suggest that the main Paleo-Tethys Ocean basin was probably opened in the Middle Cambrian. However, *Metcalfe* [2013] argued that those Early Paleozoic oceanic crust remnants from the LSSZ were too old to be formed in the Paleo-Tethys, which had been widely accepted as a Devonian to Triassic ocean. Moreover, the discovery of Silurian high-pressure granulites in the central Qiangtang block indicated the occurrence of a previous collisional event along the northern margin of the Indo-Australian Gondwana [*Zhang et al.,* 2014a]. Hence, the Early Paleozoic ophiolite remnants and the correlative high-pressure metamorphic rocks were probably records of the evolution and closure of the Early Paleozoic ocean basin (Proto-Tethyan?) along the northern margin of Gondwana. Considering the current data, the timing of ophiolites related to the Paleo-Tethys in the central Qiangtang block is constrained to be in the Permian and Carboniferous periods (Figure 11a).

5.2. Effects of Alteration and Fractionation

The oceanic crusts have been demonstrated to have generally undergone seawater hydrothermal alteration and metamorphism [e.g., *McCulloch et al.,* 1981; *Godard et al.,* 2006; *Polat and Hofmann*, 2003]. As almost all of the ophiolitic samples in this study had experienced greenschist-facies metamorphism and varying degrees of deformation (Figures 3a–3d), the potential effects of these processes were assessed by Zr versus selected element variation diagrams (Figure 8). Strong correlations between various pairs of elements (including REE

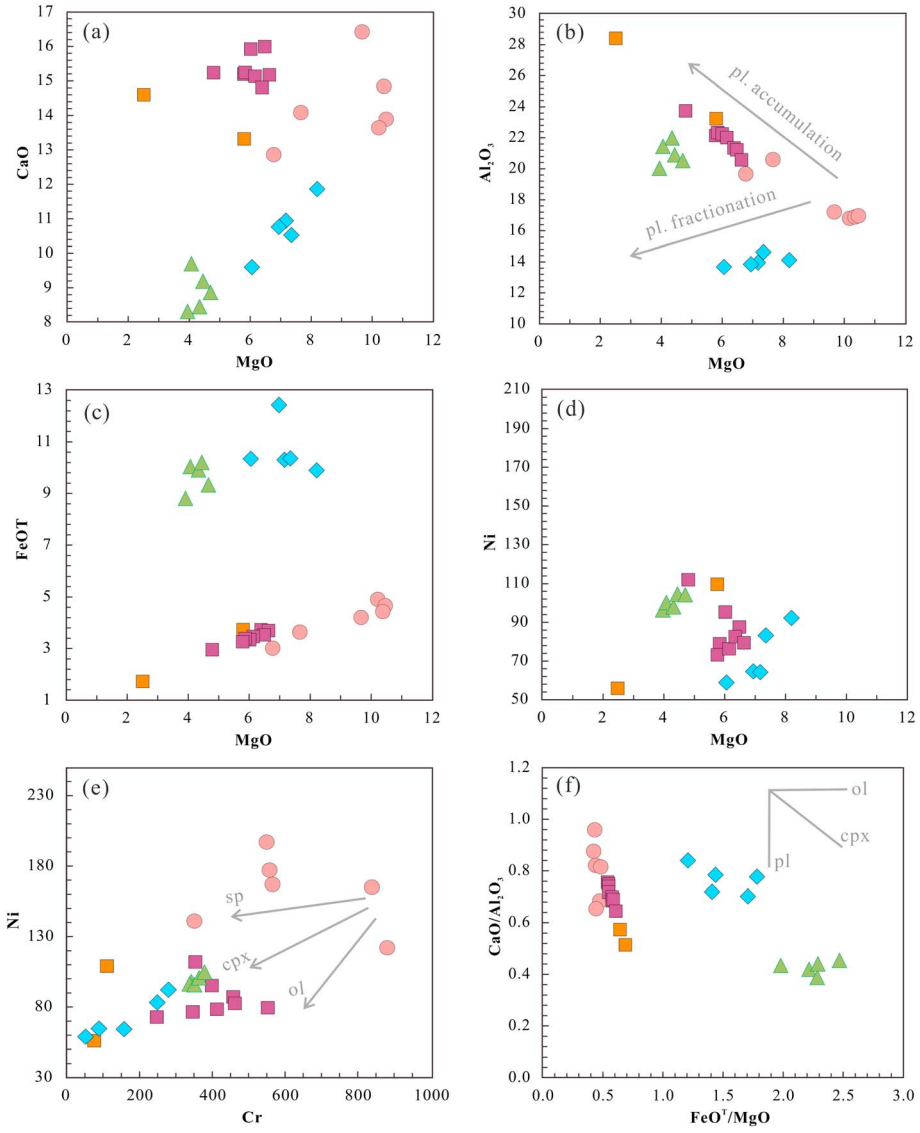

Figure 9. Harker diagrams showing chemical variations as functions of MgO (a–d), correlation diagram between Ni and Cr (e), and CaO/Al_2O_3 versus FeO^T/MgO diagram (f) for the Xiangtaohu ophiolites in the central Qiangtang, central Tibet. Pl. = plagioclase, Sp. = spinel, Cpx. = clinopyroxene, and Ol. = olivine.

(e.g., Nd and Yb), Nb, Ta, Th, Ti, V, and Zr) indicate that these elements were not disturbed significantly by alteration (Figure 8). In contrast, some large-ion-lithophile elements (LILEs, e.g., Rb and U) have been significantly modified by alteration and metamorphism (Figure 8). Therefore, these mobile elements are omitted in the discussion below.

The mafic samples from the Xiangtaohu ophiolities show variable SiO_2 and MgO contents (43.9–51.7 wt % and 2.51–10.4 wt %, respectively) and a large range of $Mg^{\#}$ values (41–81) (Table S2), implying a common fractional crystallization and/or accumulation process. In the Harker diagram (Figure 9), the metabasalt and appinitic dike samples from Permian ophiolites (Oph_1) exhibit a crude positive correlation between MgO and CaO, Cr, and Ni and also a positive correlation between Cr and Ni, indicating their parental magmas probably undergone substantial clinopyroxene and olivine fractionation [*Ma et al.*, 2015]. In contrast, the constituents of gabbros from the Permian and Carboniferous ophiolites (Oph_1 and Oph_2) are mainly controlled by the plagioclase accumulation process based on the MgO versus Al_2O_3 element, and FeO^T/MgO versus CaO/Al_2O_3 ratio variation diagrams (Figures 9e and 9f).

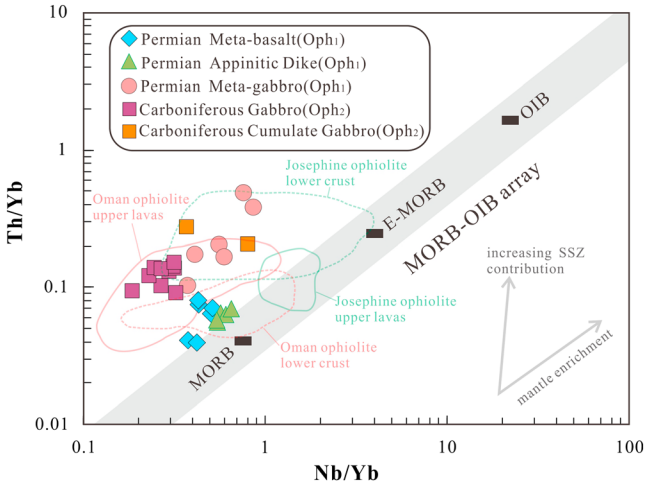

Figure 10. Th/Yb versus Nb/Yb diagram [*Pearce*, 2008] for the basaltic rocks from the Xiangtaohu ophiolites in the central Qiangtang, central Tibet. Data for the Josephine and Oman ophiolites are from *Harper* [2003a, 2003b], *Alabaster et al.* [1982], and *Godard et al.* [2003].

5.3. Carboniferous to Permian SSZ Ophiolites in Central Qiangtang

5.3.1. N-MORB-Like Affinity

All the mafic to ultramafic samples from the Carboniferous and Permian ophiolites are characterized by low REE abundances and depletion of LREE, consistent with the characteristics of N-MORB. In addition, their N-MORB-normalized elements show a very flat pattern (Figure 6). Especially for the metabasalt (Figure 6b) and appinitic dike (Figure 6d) samples from the Permian ophiolites, their N-MORB-normalized element ratios are very close to 1 (Figure 6), indicating a strong N-MORB-affinity. The Nb/Yb and Nb/Y ratios, which are largely independent of the extent of partial melting and crystal fractionation, are good tracers of mantle source composition and generally represent the degree of mantle enrichment and/or depletion [*Pearce*, 2008]. All the mafic samples in this study have very low Nb/Yb (0.19–0.86) and Nb/Y ratios (0.02–0.08), which are very close to those of N-MORB (Nb/Yb = 0.76, Nb/Y = 0.08) [*Sun and McDonough*, 1989], suggesting that they were derived from an N-MORB-like depleted mantle source. This inference is further supported by Nd isotopes. As a result of hydrothermal alteration and metamorphism, some high $^{87}Sr/^{86}Sr$ ratios of the ophiolitic rocks are not considered to be magmatic Sr isotope compositions. In contrast, Nd has been proved to be relatively immobile during alteration and metamorphism (Figure 8). The Carboniferous to Permian ophiolitic samples have relatively high $^{143}Nd/^{144}Nd$ ratios and positive $\varepsilon_{Nd}(t)$ values, indicating that these rocks were mainly derived from a highly depleted mantle source.

In summary, the whole-rock geochemical and Nd isotope compositions suggest that both the Carboniferous and Permian ophiolites from the Xiangtaohu area have strong N-MORB-like features and were mainly derived from the N-MORB-like depleted mantle source.

5.3.2. Suprasubduction-Zone Signatures

Compared to N-MORB, almost all the Carboniferous and Permian ophiolitic samples have slight enrichment of Th but depletions in Nb and Ti to varying degrees (Figures 6b, 6d, 6f, and 6h). These features could be significant suprasubduction zone (SSZ) signatures which indicate the mantle source had been influenced by subducted materials [*Metcalf and Shervais*, 2008]. The element Th is widely considered as a tracer of subducted components [*Plank and Langmuir*, 1998], and the Th/Yb ratio is also independent of the extent of partial melting and crystal fractionation. Hence, increasing Th/Yb ratio represents increasing subducted material contribution [*Elliott et al.*, 1997; *Singer et al.*, 2007]. All the Carboniferous and Permian ophiolitic samples show relatively high Th/Yb but low Ta/Yb ratios and plot above the MORB-OIB mantle array (Figure 10). Furthermore, the $\delta^{18}O$ values of zircon are relatively insensitive to magmatic differentiation [*Valley*, 2003], which can also reflect the feature of magmas. The gabbro samples (L1223-1 and L1203-1) from both Carboniferous and Permian ophiolites yielded average $\delta^{18}O_{zircon}$ values of 5.49 ± 0.18‰ and 5.90 ± 0.24‰, respectively. These values are within or slightly higher than those of the unaltered MORB $\delta^{18}O_{zircon}$ value (5.2 ± 0.5%) [*Grimes et al.*, 2011], further implying subducted material contribution.

It is noteworthy that the SSZ signature is increasingly apparent from upper to lower lava sequence in the ophiolites from the Qiangtang block. Mafic rocks of the upper lava sequence (metabasalts and appinitic dikes) of the Permian ophiolites have high TiO_2 values (1.08–1.89 wt %), high field strength elements (HFSE) (insignificant Nb and Ti negative anomalies), REE concentrations, and lower Th/Nb ratios, which feature is more approximate to N-MORB [*Sun and McDonough*, 1989]. Although the Carboniferous ophiolites in the Xiangtaohu area are missing the upper lava sequence, the basalts from coeval ophiolites in the Gangma Co (357–354 Ma) and Guoganjianianshan (345 Ma) areas also have some SSZ signatures and are

similar to N-MORB to E-MORB [*Zhai et al.,* 2013]. In contrast, the lower lava sequence (gabbros and cumulate gabbros) in both Permian and Carboniferous ophiolites from the Xiaongtaohu area, as well as the Carboniferous ophiolites from the Gangma Co and Guoganjianianshan areas [*Zhai et al.,* 2013], have low TiO_2 values (0.14–0.31 wt %), HFSE (obvious Nb-Ti negative anomalies), and REE concentrations, but high Th/Nb ratios, which are indicative of strong SSZ signatures.

In summary, the Permian and Carboniferous ophiolites documented in the central Qiangtang block exhibit both suprasubduction zone-like and MORB-like geochemical features, which are similar to many typical SSZ-type ophiolites in the world, such as the Josephine ophiolite of northern California and southern Oregon, and Oman ophiolites (Figure 10) [e.g., *Harper,* 2003a, 2003b; *Alabaster et al.,* 1982; *Godard et al.,* 2003; *Metcalf and Shervais*, 2008]. Their compositional variation trend from upper to lower lava sequence is much closer to that of Josephine ophiolites (Figure 10).

5.3.3. Evidence of Crystallization Sequences and Hydrous Magmas

SSZ ophiolites have been recognized from the exposed ophiolites in the world for over 40 years [*Miyashiro*, 1973; *Pearce et al.,* 1984], and it is widely accepted that most exposed ophiolites were formed in the suprasubduction zone (SSZ) settings, not at the mid-ocean ridge spreading centers [e.g., *Shervais*, 2001; *Metcalf and Shervais*, 2008; *Pearce*, 2008; *Wakabayashi et al.,* 2010]. Alternatively, some authors have argued that most ophiolites with SSZ signatures were formed at the mid-ocean ridges that tap the upper mantle sources previously modified by subduction [*Moores et al.,* 2000]. Hence, besides geochemistry and isotope data, further evidence is needed to confirm the tectonic settings of ophiolites. Experimental data show that compared to the dry environment at the mid-ocean ridges for magma generation and crystallization, water plays a key role in the genesis and evolution of subduction-zone magmas [*Sisson and Grove*, 1993; *Metcalf and Shervais*, 2008]. The wet subduction-zone magmas are characterized by the crystallization sequence of olivine-clinopyroxene-plagioclase, instead of the dry MORB crystallization sequence of olivine-plagioclase-clinopyroxene [e.g., *Pearce et al.,* 1984; *Hébert and Laurent*, 1990]. The well-preserved Carboniferous ultramafic to mafic cumulate rocks (pyroxene peridotite- pyroxenite -cumulate gabbro) in the Xiangtaohu area (Figures 2f–2h and 3f–3h) reveal distinct SSZ-type cumulate sequences (pyroxene before plagioclase), indicating wet magmas. Moreover, the identification of appinitic dikes in the Permian ophiolites provides direct evidence for a high water content in the magma [*Metcalf and Shervais*, 2008; *Murphy*, 2013].

In conclusion, the Permian and Carboniferous ophiolites from the central Qiangtang block were derived from an N-MORB-like mantle source with variable intensities of SSZ signatures and were characterized by crystallization sequences from wet magmas, suggesting that they are typical SSZ-affinity ophiolites.

6. Tectonic Implications

Growing evidence indicates that the central Tibet is a key locality for identifying the remnants of the main Paleo-Tethys Ocean and for rebuilding its evolutionary history [*Li*, 1987; *Li and Zheng*, 1993; *Zhai et al.,* 2011a, 2011b, 2013; *Metcalfe*, 2013; *Kapp et al.,* 2000; *Pullen et al.,* 2011]. Although low-temperature and high-pressure metamorphic rocks have been documented to occur in the LSSZ [*Li et al.,* 2006; *Zhang et al*., 2006a; *Zhai et al.,* 2011a, 2011b], some researchers still consider them as a part of the Songpan-Ganzi accretionary mélange that was underthrusted along the Jinsha suture [e.g., *Kapp et al.,* 2000; *Pullen et al.,* 2011] for lacking crucial evolution records of the ocean crust. The presence of Permian and Carboniferous SSZ ophiolites in the Xiangtaohu area, as well as that of the Carboniferous ophiolites in the Gangma Co and Guoganjianianshan areas [*Zhai et al.,* 2013], provide robust evidence for the existence of an ancient ocean basin (Figure 11). Moreover, the occurrence of the SSZ ophiolites indicates that the ancient oceanic crust had undergone a series of complex tectonic evolutional processes, including intraoceanic subduction, continued hinge rollback, upper plate extension, formation of the SSZ crust, and ophiolite emplacement by obduction or accretionary uplift [e.g., *Stern and Bloomer*, 1992; *Shervais*, 2001; *Metcalf and Shervais*, 2008]. The Permian and Carboniferous SSZ ophiolites, combined with the Late Devonian and Permian pelagic radiolarian cherts [*Zhu et al.,* 2006], further confirm that the LSSZ represent a long-lived ancient ocean basin. These evolution records of the ocean crust correspond exactly with those from the main Paleo-Tethys suture zone, such as the Devonian to Permian SSZ ophiolites in the Changning-Menglian suture zone [*Jian et al.,* 2009a, 2009b; *Fang et al.,* 1994] and the Devonian to Triassic Pelagic cherts and MORB basalts in the Chiang Mai-Inthanon suture zone (reviewed by *Zhang et al.* [2008] and *Metcalfe* [2013]).

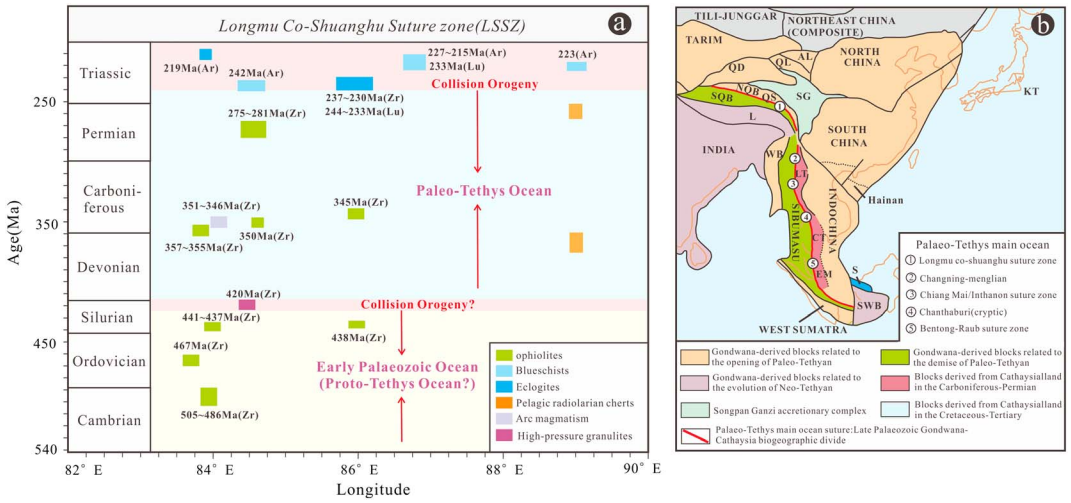

Figure 11. (a) Simplified chart showing the ages of magmatic and metamorphic events which provide robust evidence for the existence and evolution of the Paleo-Tethys Ocean and the northeastern margin of Gondwana. (b) Distribution of the main suture zones of the Paleo-Tethys Ocean and Gondwana-derived continental blocks related to the opening and demise of Paleo-Tethys Ocean (modified from *Metcalfe* [2013]). Lu = garnet Lu–Hf isochron dating, Zr = zircon U-Pb dating (SHRIMP and LA-ICP-MS), and Ar = $^{40}Ar/^{39}Ar$ isochron dating for mineral (glaucophane and phengite), WB = West Burma, SWB = South West Borneo, S = Semitau, L = Lhasa, SQT = South Qiangtang, NQT = North Qiangtang, QS = Qamdo-Simao, SI = Simao, SG = Songpan Ganzi accretionary complex, QD = Qaidam, QI = Qilian, AL = Ala Shan, KT = Kurosegawa Terrane, LT = Lincang arc Terrane, CT = Chanthaburi arc Terrane, and EM = East Malaya. Data are from *Zhai et al.* [2009, 2010, 2011a, 2013, 2016], *Pullen et al.* [2008], *Zhang et al.* [2014a, 2014c], *Bao et al.* [1999], *Hu et al.* [2014], *Li et al.* [2008], *Zhu et al.* [2006], *Jiang et al.* [2015], *Kapp et al.* [2003], and *Tang and Zhang* [2014].

Tectonostratigraphic and paleontological data show the highly contrasting juxtaposition of the cool faunas of Gondwana affinities with the warm-climate biotas of Cathaysian affinities in Carboniferous to Permian strata on either side of the LSSZ [*Metcalfe*, 1994, 2013; *Li and Zheng*, 1993; *Fan et al.,* 2014; *Peng et al.,* 2014]. Furthermore, provenance analysis results reveal that the maximum depositional ages of samples from the NQB (north of the LSSZ) are very close to their major age peak and to the ages of adjacent arc magmatic rocks [e.g., *Peng et al.,* 2014; *Jiang et al.,* 2015], implying an active continental margin setting associated with the northward subduction of the Paleo-Tethyan Oceanic lithosphere. Conversely, the Carboniferous-Permian samples from the SQB (south of LSSZ), their minimum crystallization age of the zircons are obviously older than their depositional ages [*Gehrels et al.,* 2011; *Fan et al.,* 2014], suggesting a passive continental setting [*Cawood et al.,* 2012]. The LT-HP metamorphic rocks are important indicators of collision orogeny following the closure of an ocean basin [*O'Brien and Rötzler*, 2003; *Ernst and Liou*, 2008]. The timing of eclogites and blueschists (244–223 Ma) located in the LSSZ marks the closure of an ancient ocean basin in the Middle–Late Triassic (Figure 11a) [*Pullen et al.,* 2008; *Zhai et al.,* 2011a, 2011b]. Taken together, the above evidence suggests that the LSSZ should represent the main suture of the Paleo-Tethys Ocean, which existed and evolved probably from Devonian to Middle–Late Triassic.

The LSSZ in central Tibet, probably along with the Changning-Menglian, Chiang Mai-Inthanon, and Bentong-Raub suture zones, constituted the main suture of the Paleo-Tethys Ocean (Figure 11b) (reviewed by *Metcalfe* [2013]). These suture zones preserved a significant record of fossil oceanic evolution, Gondwana dispersion, and early Asian accretion history. In the early Paleozoic, most blocks (e.g., South China, North China, Indochina, and Tarim blocks) which formed present day the East and/or Southeast Asia were located along the Indo-Australian margin of northeastern Gondwana [*Metcalfe*, 1994, 2013; *Yao et al.,* 2014]. The eastern Paleo-Tethyan Ocean was initially opened during the Early Devonian in response to the detachment of the ribbon-like Asiatic Hunic superterrane from the northern margin of Gondwana [*Stampfli and Borel*, 2002; *von Raumer et al.,* 2002; *Ferrari et al.,* 2008; *Lehmann et al.,* 2013; *Metcalfe*, 2013]. These blocks migrated northward to be a part of Eurasia in response to the expansion of the Paleo-Tethys Ocean [*Metcalfe*, 1994, 2013]. The Middle–Late Triassic collision between Cimmerian Continent (e.g., south Qiangtang and Sino-Siam-Burma-Malaya-Sumatra) and Eurasia resulted in the closure of the eastern Paleo-Tethyan Ocean and

the formation of the basic framework for the East and/or Southeast Asia (Figure 11b). The opening and closing of the Paleo-Tethys Ocean dominated the origin and early accretionary history of the East and/or Southeast Asia.

7. Conclusions

1. Detailed geological investigations and zircon U-Pb dating reveal that the Xiangtaohu ophiolites from the central Qiangtang block are composed of a suite of Early Permian (281–275 Ma) ophiolites with nearly complete Penrose sequence and a suite of Early Carboniferous (circa 350 Ma) ophiolite remnants containing only part of the lower oceanic crust.
2. Geochemical and Sr-Nd-O isotopic data show that the Permian and Carboniferous ophiolites were derived from an N-MORB-like mantle source with varying intensity of SSZ signatures and were characterized by crystallization sequences from wet magmas, suggesting typical SSZ-affinity ophiolites.
3. Permian and Carboniferous SSZ ophiolites in the central Qiangtang provide robust evidence for the existence and evolution of an ancient ocean basin. These ophiolites, together with pelagic radiolarian cherts, eclogites, and blueschists located along the LSSZ, represent the remnants of the main Paleo-Tethys Ocean.

Acknowledgments
We are grateful to Editor John Geissman, Associate Editor Andrei Khudoley, Ian Metcalfe, and an anonymous reviewer for their constructive and helpful reviews. We thank Li Su, Wen-Chun Ge, and Wen Zeng for their assistance in the LA-ICP-MS dating and Sr-Nd isotopic analyses. This study was jointly supported by the Strategic Priority Research Program (B) of the Chinese Academy of Sciences (grant XDB03010600), the National Natural Science Foundation of China (41372066, 41502054, 41025006 and 41421062), the China Postdoctoral Science Foundation funded project (grant 2015M572374), talent project of Guangdong Province (2014TX01Z079), and GIGCAS 135 project 135TP201601. This is contribution IS-2267 from the GIGCAS.

References

Alabaster, T., J. A. Pearce, and J. Malpas (1982), The volcanic stratigraphy and petrogenesis of the Oman ophiolite complex, *Contrib. Mineral. Petrol.*, *81*(3), 168–183.

Bao, P. S., X. C. Xiao, J. Wang, C. Li, and K. Hu (1999), Blue schist belt of Shuanghu area in Center-Northern Xizang (Tibet) and its tectonic Implications [in Chinese with English abstract], *Acta Geol. Sin.*, *73*(4), 302–314.

Cawood, P. A., C. J. Hawkesworth, and B. Dhuime (2012), Detrital zircon record and tectonic setting, *Geology*, *40*(10), 875–878.

Coleman, R. G. (1977), *Ophiolites—Ancient Oceanic Lithosphere?*, *Miner. and Rocks*, vol. 12, 229 pp., Springer, New York.

Deng, X. G., L. Ding, X. H. Liu, Y. An, P. A. Kapp, M. A. Murphy, and C. E. Manning (2000), Discovery of blueschists in Gangmar–Taoxing Co area, central Qiangtang, northern Tibet [in Chinese with English abstract], *Acta Geol. Sin.*, *35*(2), 227–232.

Dewey, J. F., and J. M. Bird (1971), Origin and emplacement of ophiolite suite—Appalachian ophiolites in Newfoundland, *J. Geophys. Res.*, *76*, 3179–3206, doi:10.1029/JB076i014p03179.

Dilek, Y. (2003), Ophiolite concept and its evolution, in *Ophiolite Concept and the Evolution of Geological Thought*, *Spec. Pap.*, vol. 373, edited by Y. Dilek and S. Newcomb, pp. 1–16, Geol. Soc. of Am., Boulder, Colo.

Elliott, T., T. Plank, A. Zindler, W. White, and B. Bourdon (1997), Element transport from slab to volcanic front at the Mariana arc, *J. Geophys. Res.*, *102*, 14,991–15,019, doi:10.1029/97JB00788.

Ernst, W. G., and J. G. Liou (2008), High- and ultrahigh-pressure metamorphism: Past results and future prospects, *Am. Mineral.*, *93*, 1771–1786.

Fan, J. J., C. Li, M. Wang, C. M. Xie, and W. Xu (2014), Features, provenance, and tectonic significance of Carboniferous–Permian glacial marine diamictites in the Southern Qiangtang–Baoshan block, Tibetan Plateau, *Gondwana Res.*, doi:10.1016/j.gr.2014.10.015.

Fang, N., B. Liu, Q. Feng, and J. Jia (1994), Late Palaeozoic and Triassic deep-water deposits and tectonic evolution of the Palaeotethys in the Changning-Menglian and Lancangjiang belts, southwestern Yunnan, *J. Southeast Asian Earth Sci.*, *9*, 363–374.

Ferrari, O. M., C. Hochard, and G. M. Stampfli (2008), An alternative plate tectonic model for the Palaeozoic–Early Mesozoic Palaeotethyan evolution of Southeast Asia (Northern Thailand–Burma), *Tectonophysics*, *451*, 346–365.

Gehrels, G., et al. (2011), Detrital zircon geochronology of pre–Tertiary strata in the Tibetan–Himalayan orogen, *Tectonics*, *30*, TC5016, doi:10.1029/2011TC002868.

Godard, M., J. M. Dautria, and M. Perrin (2003), Geochemical variability of the Oman ophiolite lavas: Relationship with spatial distribution and paleomagnetic directions, *Geochem. Geophys. Geosyst.*, *4*(6), 8609, doi:10.1029/2002GC000452.

Godard, M., D. Bosch, and F. Einaudi (2006), A MORB source for low-Ti magmatism in the Semail ophiolite, *Chem. Geol.*, *234*, 58–78.

Grimes, C. B., T. Ushikubo, B. E. John, and J. W. Valley (2011), Uniformly mantle-like δ18O in zircons from oceanic plagiogranites and gabbros, *Contrib. Mineral. Petrol.*, *161*(1), 13–33.

Harper, G. D. (2003a), Fe-Ti basalts and propagating-rift tectonics in the Josephine Ophiolite, *Geol. Soc. Am. Bull.*, *115*(7), 771–787.

Harper, G. D. (2003b), Tectonic implications of boninite, arc tholeiite, and MORB magma types in the Josephine ophiolite, California, Oregon, in *Ophiolites in Earth History*, edited by Y. Dilek and P. T. Robinson, *Geol. Soc. London, Spec. Publ.*, *218*, 207–230.

Hébert, R., and R. Laurent (1990), Mineral chemistry of the plutonic section of the Troodos ophiolite: New constraints for genesis of arc-related ophiolites, in *Ophiolites: Oceanic Crustal Analogues*, pp. 149–163, Geol. Surv. Cyprus, Nicosia.

Hoskin, P. W. O., and L. P. Black (2000), Metamorphic zircon formation by solid-state recrystallization of protolith igneous zircon, *J. Metamorph. Geol.*, *18*(4), 423–439.

Hu, P. Y., C. Li, Y. W. Wu, C. M. Xie, M. Wang, and J. Li (2014), Opening of the Longmu Co–Shuanghu–Lancangjiang ocean: Constraints from plagiogranites, *Chin. Sci. Bull.*, *59*(25), 3188–3199.

Jian, P., D. Y. Liu, A. Kroner, Q. Zhang, Y. Z. Wang, X. M. Sun, and W. Zhang (2009a), Devonian to Permian plate tectonic cycle of the Paleo-Tethys Orogen in southwest China (I): Geochemistry of ophiolites, arc/back-arc assemblages and within-plate igneous rocks, *Lithos*, *113*(3–4), 748–766.

Jian, P., D. Y. Liu, A. Kroner, Q. Zhang, Y. Z. Wang, X. M. Sun, and W. Zhang (2009b), Devonian to Permian plate tectonic cycle of the Paleo-Tethys Orogen in southwest China (II): Insights from zircon ages of ophiolites, arc/back-arc assemblages and within-plate igneous rocks and generation of the Emeishan CFB province, *Lithos*, *113*(3–4), 767–784.

Jiang, Q. Y., C. Li, L. Su, P. Y. Hu, C. M. Xie, and H. Wu (2015), Carboniferous arc magmatism in the Qiangtang area, northern Tibet: Zircon U–Pb ages, geochemical and Lu–Hf isotopic characteristics, and tectonic implications, *J. Asian Earth Sci.*, *100*, 132–144.

Kapp, P., A. Yin, C. E. Manning, M. Murphy, T. M. Harrison, M. Spurlin, D. Lin, X. G. Deng, and C. M. Wu (2000), Blueschist-bearing metamorphic core complexes in the Qiangtang block reveal deep crustal structure of northern Tibet, *Geology*, *28*(1), 19–22.

Kapp, P., A. Yin, C. E. Manning, T. M. Harrison, M. H. Taylor, and L. Ding (2003), Tectonic evolution of the early Mesozoic blueschist-bearing Qiangtang metamorphic belt, central Tibet, *Tectonics*, *22*(4), 1043, doi:10.1029/2002TC001383.

Lehmann, B., X. Zhao, M. Zhou, A. Du, J. Mao, P. Zeng, F. H. Kunst, and K. Heppe (2013), Mid-Silurian back-arc spreading at the northeastern margin of Gondwana: The Dapingzhang dacite-hosted massive sulfide deposit, Lancangjiang zone, southwestern Yunnan, China, *Gondwana Res.*, *24*(2), 648–663.

Li, C. (1987), The Longmu Co-Shuanghu-Lanchangjiang plate suture and the north boundary of distribution of Gondwana affinity Permian-Carboniferous system in northern Tibet, China [in Chinese with English abstract], *J. Changchun Univ. Earth Sci.*, *17*(2), 155–166.

Li, C., and A. Zheng (1993), Paleozoic stratigraphy in the Qiangtang region of Tibet: Relations of the Gondwana and Yangtze continents and ocean closure near the end of the Carboniferous, *Int. Geol. Rev.*, *35*(9), 797–804.

Li, C., L. R. Cheng, K. Hu, Z. R. Yang, and Y. R. Hong (1995), *Study on the Paleo-Tethys Suture Zone of Longmu Co-Shuanghu, Tibet* [in Chinese with English abstract], Geol. House, Beijing.

Li, C., Q. G. Zhai, Y. S. Dong, and X. P. Huang (2006), Discovery of eclogite and its geological significance in Qiangtang area, central Tibet, *Chin. Sci. Bull.*, *51*(9), 1095–1100.

Li, C., Y. S. Dong, Q. G. Zhai, L. Q. Wang, Q. R. Yan, Y. W. Wu, and T. T. He (2008), Discovery of Eopaleozoic ophiolite in the Qiangtang of Tibet Plateau: Evidence from SHRIMP U–Pb dating and its tectonic implications [in Chinese with English abstract], *Acta Petrol. Sin.*, *24*(1), 31–36.

Ma, L., Q. Wang, D. A. Wyman, Z. Q. Jiang, F. Y. Wu, X. H. Li, J. H. Yang, G. N. Gou, and H. F. Guo (2015), Late Cretaceous back-arc extension and arc system evolution in the Gangdese area, southern Tibet: Geochronological, petrological, and Sr-Nd-Hf-O isotopic evidence from Dagze diabases, *J. Geophys. Res. Solid Earth*, *120*, 6159–6181, doi:10.1002/2015JB011966.

McCulloch, M. T., R. T. Gregory, G. J. Wasserburg, and H. P. Taylor Jr. (1981), Sm–Nd, Rb–Sr, and $^{18}O/^{16}O$ isotopic systematics in an oceanic crustal section: Evidence from the Samail ophiolite, *J. Geophys. Res.*, *86*, 2721–2735, doi:10.1029/JB086iB04p02721.

Metcalf, R. V., and J. W. Shervais (2008), Suprasubduction-zone ophiolites: Is there really an ophiolite conundrum?, *Geol. Soc. Am. Spec. Pap.*, *438*, 191–222.

Metcalfe, I. (1994), Gondwanaland origin, dispersion, and accretion of East and Southeast Asian continental terranes, *J. South Am. Earth Sci.*, *7*, 333–347.

Metcalfe, I. (2013), Gondwana dispersion and Asian accretion: Tectonic and palaeogeographic evolution of eastern Tethys, *J. Asian Earth Sci.*, *66*, 1–33.

Miyashiro, A. (1973), The Troodos ophiolitic complex was probably formed in an island arc, *Earth Planet. Sci. Lett.*, *19*(2), 218–224.

Miyashiro, A. (1974), Volcanic rock series in island arcs and active continental margins, *Am. J. Sci.*, *274*(4), 321–355.

Moores, E. M., L. H. Kellogg, and Y. Dilek (2000), Tethyan ophiolites, mantle convection, and tectonic "historical contingency": A resolution of the "ophiolite conundrum", *Spec. Pap. Geol. Soc. Am.*, *349*, 3–12.

Murphy, J. B. (2013), Appinite suites: A record of the role of water in the genesis, transport, emplacement and crystallization of magma, *Earth Sci. Rev.*, *119*, 35–59.

O'Brien, P. J., and J. Rötzler (2003), High-pressure granulites: Formation, recovery of peak conditions and implications for tectonics, *J. Metamorph. Geol.*, *21*(1), 3–20.

Pearce, J. A. (2008), Geochemical fingerprinting of oceanic basalts with applications to ophiolite classification and the search for Archean oceanic crust, *Lithos*, *100*(1–4), 14–48.

Pearce, J. A., S. J. Lippard, and S. Roberts (1984), Characteristics and tectonic significance of supra-subduction zone ophiolites, *Geol. Soc. London Spec. Publ.*, *16*(1), 77–94.

Peng, H., C. Li, C. M. Xie, M. Wang, Q. Y. Jiang, and J. W. Chen (2014), Riwanchaka group in central Qiangtang Basin, the Tibetan Plateau: Evidence from detrital zircons [in Chinese with English abstract], *Geol. Bull. China*, *33*(11), 1715–1727.

Penrose Conference Participants (1972), Penrose field conference on ophiolites, *Geotimes*, *17*, 24–25.

Plank, T., and C. H. Langmuir (1998), The chemical composition of subducting sediment and its consequences for the crust and mantle, *Chem. Geol.*, *145*, 325–394.

Polat, A., and A. W. Hofmann (2003), Alteration and geochemical patterns in the 3.7–3.8 Ga Isua greenstone belt, West Greenland, *Precambrian Res.*, *126*(3), 197–218.

Pullen, A., P. Kapp, G. E. Gehrels, J. D. Vervoort, and L. Ding (2008), Triassic continental subduction in central Tibet and Mediterranean-style closure of the Paleo-Tethys Ocean, *Geology*, *36*(5), 351–354.

Pullen, A., P. Kapp, G. E. Gehrels, L. Ding, and Q. H. Zhang (2011), Metamorphic rocks in central Tibet: Lateral variations and implications for crustal structure, *Geol. Soc. Am. Bull.*, *123*, 585–600.

Shervais, J. W. (2001), Birth, death, and resurrection: The life cycle of suprasubduction zone ophiolites, *Geochem. Geophys. Geosyst.*, *2*(1), 1010, doi:10.1029/2000GC000080.

Singer, B. S., B. R. Jicha, W. P. Leeman, N. W. Rogers, M. F. Thirlwall, J. Ryan, and K. E. Nicolaysen (2007), Along-strike trace element and isotopic variation in Aleutian Island arc basalt: Subduction melts sediments and dehydrates serpentine, *J. Geophys. Res.*, *112*, B06206, doi:10.1029/2006JB004897.

Sisson, T. W., and T. L. Grove (1993), Experimental investigations of the role of H_2O in calc-alkaline differentiation and subduction zone magmatism, *Contrib. Mineral. Petrol.*, *113*(2), 143–166.

Stampfli, G. M., and G. D. Borel (2002), A plate tectonic model for the Paleozoic and Mesozoic constrained by dynamic plate boundaries and restored synthetic oceanic isochrones, *Earth Planet. Sci. Lett.*, *196*, 17–33.

Stern, R. J., and S. H. Bloomer (1992), Subduction zone infancy: Examples from the Eocene Izu-Bonin-Mariana and Jurassic California arcs, *Geol. Soc. Am. Bull.*, *104*(12), 1621–1636.

Sun, S. S., and W. F. McDonough (1989), Chemical and isotopic systematics of oceanic basalts: Implications for mantle composition and processes, *Geol. Soc. London Spec. Publ.*, *42*, 313–345.

Tang, X. C., and K. J. Zhang (2014), Lawsonite-and glaucophane-bearing blueschists from NW Qiangtang, northern Tibet, China: Mineralogy, geochemistry, geochronology, and tectonic implications, *Int. Geol. Rev.*, *56*(2), 150–166.

Valley, J. W. (2003), Oxygen isotopes in zircon, in *Zircon: Reviews in Mineralogy and Geochemistry*, vol. 53, edited by J. M. Hanchar and P. W. O. Hoskin, pp. 343–385, Mineral. Soc. of Am., Washington, D. C.

Von Raumer, J., G. Stampfli, G. Borel, and F. Bussy (2002), Organization of pre-Variscan basement areas at the north-Gondwanan margin, *Int. J. Earth Sci.*, *91*, 35–52.

Wakabayashi, J., A. Ghatak, and A. R. Basu (2010), Suprasubduction-zone ophiolite generation, emplacement, and initiation of subduction: A perspective from geochemistry, metamorphism, geochronology, and regional geology, *Geol. Soc. Am. Bull.*, *122*(9–10), 1548–1568.

Winchester, J. A., and P. A. Floyd (1977), Geochemical discrimination of different magma series and their differentiation products using immobile elements, *Chem. Geol.*, *20*(4), 325–343.

Xu, J. F., and P. R. Castillo (2004), Geochemical and Nd–Pb isotopic characteristics of the Tethyan asthenosphere: Implications for the origin of the Indian Ocean mantle domain, *Tectonophysics*, *393*(1–4), 9–27.

Yao, W. H., Z. X. Li, W. X. Li, X. H. Li, and J. H. Yang (2014), From Rodinia to Gondwanaland: A tale of detrital zircon provenance analyses from the southern Nanhua Basin, South China, *Am. J. Sci.*, *314*(1), 278–313.

Yin, A., and T. M. Harrison (2000), Geologic evolution of the Himalayan–Tibetan orogen, *Annu. Rev. Earth Planet. Sci.*, *28*, 211–280.

Zhai, Q. G., C. Li, J. Wang, W. Chen, and Y. Zhang (2009), Petrology, mineralogy and $^{40}Ar/^{39}Ar$ chronology for Rongma blueschist from central Qiangtang, northern Tibet [in Chinese with English abstract], *Acta Petrol. Sin.*, *25*(9), 2281–2288.

Zhai, Q. G., J. Wang, C. Li, and L. Su (2010), SHRIMP U–Pb dating and Hf isotopic analyses of Middle Ordovician meta-cumulate gabbro in central Qiangtang, northern Tibetan plateau, *Sci. China, Ser. D: Earth Sci.*, *53*(5), 657–664.

Zhai, Q. G., R. Y. Zhang, B. M. Jahn, C. Li, S. G. Song, and J. Wang (2011a), Triassic eclogites from central Qiangtang, northern Tibet, China: Petrology, geochronology and metamorphic P–T path, *Lithos*, *125*(1–2), 173–189.

Zhai, Q. G., B. M. Jahn, R. Y. Zhang, J. Wang, and L. Su (2011b), Triassic subduction of the Paleo–Tethys in northern Tibet, China: Evidence from the geochemical and isotopic characteristics of eclogites and blueschists of the Qiangtang Block, *J. Asian Earth Sci.*, *42*(6), 1356–1370.

Zhai, Q. G., B. M. Jahn, J. Wang, L. Su, X. X. Mo, K. L. Wang, S. H. Tang, and H. Y. Lee (2013), The Carboniferous ophiolite in the middle of the Qiangtang terrane, Northern Tibet: SHRIMP U–Pb dating, geochemical and Sr–Nd–Hf isotopic characteristics, *Lithos*, *168*, 186–199.

Zhai, Q. G., B. M. Jahn, J. Wang, P. Y. Hu, S. L. Chung, H. Y. Lee, S. H. Tang, and Y. Tang (2016), Oldest Paleo-Tethyan ophiolitic mélange in the Tibetan plateau, *Geol. Soc. Am. Bull.*, *128*(3–4), 355–373.

Zhang, K. J., J. X. Cai, Y. X. Zhang, and T. P. Zhao (2006a), Eclogites from central Qiangtang, northern Tibet (China) and tectonic implications, *Earth Planet. Sci. Lett.*, *245*(3), 722–729.

Zhang, K. J., Y. X. Zhang, B. Li, Y. T. Zhu, and R. Z. Wei (2006b), The blueschist-bearing Qiangtang metamorphic belt (northern Tibet, China) as an in situ suture zone: Evidence from geochemical comparison with the Jinsa suture, *Geology*, *34*, 493–496.

Zhang, Q., C. Y. Wang, D. Liu, P. Jian, Q. Qian, G. Zhou, and P. T. Robinson (2008), A brief review of ophiolites in China, *J. Asian Earth Sci.*, *32*(5), 308–324.

Zhang, X. Z., Y. S. Dong, C. Li, M. R. Deng, L. Zhang, and W. Xu (2014a), Silurian high–pressure granulites from Central Qiangtang, Tibet: Constraints on early Paleozoic collision along the northeastern margin of Gondwana, *Earth Planet. Sci. Lett.*, *405*, 39–51.

Zhang, X. Z., Y. S. Dong, C. Li, C. M. Xie, M. Wang, M. R. Deng, and L. Zhang (2014b), A record of complex histories from oceanic lithosphere subduction to continental subduction and collision: Constraints on geochemistry of eclogite and blueschist in Central Qiangtang, Tibetan Plateau [in Chinese with English abstract], *Acta Petrol. Sin.*, *30*(10), 2821–2834.

Zhang, X. Z., Y. S. Dong, C. Li, M. R. Deng, L. Zhang, and W. Xu (2014c), Tectonic setting and petrogenesis mechanism of late Triassic magmatism in Central Qiangtang, Tibetan Plateau: Take the Xiangtaohu pluton in the Hongjishan region as an example [in Chinese with English abstract], *Acta Petrol. Sin.*, *30*(2), 547–564.

Zhang, Y. C., T. X. Yuan, and Q. G. Zhai (2009), A preliminary report of the fieldtrip on the Carboniferous–Permian sequences in the north and south of the Longmu Co-Shuanghu suture zone, Northern Tibet in May and June, *Permophiles*, *53*, 5–7.

Zhu, D. C., Z. D. Zhao, Y. Niu, Y. Dilek, Z. Q. Hou, and X. X. Mo (2013), The origin and pre-Cenozoic evolution of the Tibetan Plateau, *Gondwana Res.*, *23*(4), 1429–1454.

Zhu, T. X., Q. Y. Zhang, H. Dong, Y. J. Wang, Y. S. Yu, and X. T. Feng (2006), Discovery of the Late Devonian and Late Permian radiorian cherts in tectonic melanges in the Cedo Caka area, Shuanghu, northern Tibet, China [in Chinese with English abstract], *Geol. Bull. China*, *25*(12), 1413–1418.